SIAM J. SCI. COMPUT.
Vol. 28, No. 5, pp. 1716–1729

A PSEUDOSPECTRAL FICTITIOUS POINT METHOD FOR HIGH ORDER INITIAL-BOUNDARY VALUE PROBLEMS*

BENGT FORNBERG†

Abstract. When pseudospectral approximations are used for space derivatives, one often encounters spurious eigenvalues. These can lead to severe time stepping difficulties for PDEs. This is especially the case for equations with high order derivatives in space, requiring multiple conditions at one or both boundaries. We note here that a very simple-to-implement fictitious point approach circumvents most of these difficulties. The new approach is tested on the Kuramoto–Sivashinsky equation and on a dispersive linear PDE featuring a time-space corner singularity.

Key words. spurious eigenvalues, PDE, pseudospectral method, Kuramoto–Sivashinsky equation, time-space corner singularities

AMS subject classification. 65M70

DOI. 10.1137/040611252

1. Introduction.

PDEs with high derivatives in space typically require multiple conditions at one or more of its boundaries, as noted in Table 1.1. Implementation of one Dirichlet condition at a boundary is straightforward when using a Chebyshev-type spectral method. This paper discusses how to best implement additional conditions.

The third order linear initial-boundary value (IBV) problem

$$\begin{cases} \text{PDE} & u_t = u_{xxx}, \\ \text{IC} & u(x,0) = f(x), \\ \text{BC} & u(\pm L, t) = 0,\ u_x(-L,t) = 0 \end{cases} \tag{1.1}$$

can be used to illustrate this topic. A numerical methods-of-lines (MOL) time stepping method for (1.1) will be stable if and only if the spatial differentiation operator is such that, when instead applied to the eigenvalue problem

$$\begin{cases} \text{ODE} & u_{xxx} = \lambda u, \\ \text{BC} & u(\pm L) = 0,\ u_x(-L) = 0, \end{cases} \tag{1.2}$$

the quantity $\xi = \lambda \Delta t$ for all the eigenvalues λ fall within the time stepping method's stability domain.

For the problem (1.2), the true eigenvalues are all real and negative. They are given by the roots to

$$e^{3L\lambda^{1/3}} - 2\sin\left(\sqrt{3}L\lambda^{1/3} + \frac{\pi}{6}\right) = 0 \tag{1.3}$$

(omitting $\lambda = 0$), and can be approximated very closely by

$$\lambda_k \approx -\left[\frac{\left(k+\frac{1}{6}\right)\pi}{\sqrt{3}L}\right]^3, \quad k = 1, 2, \ldots. \tag{1.4}$$

*Received by the editors July 7, 2004; accepted for publication (in revised form) April 27, 2006; published electronically October 16, 2006. This work was supported by NSF grants DMS-0309803 and DMS-0611681.

http://www.siam.org/journals/sisc/28-5/61125.html

†Department of Applied Mathematics, University of Colorado, 526 UCB, Boulder, CO 80309 (fornberg@colorado.edu).

TABLE 1.1
Number of conditions needed at each boundary for some time dependent PDEs in order to form well-posed IBV problems.

PDE		Number of conditions needed	
		Left side	Right side
$u_t = u_x$		0	1
$u_t = u_{xx}$		1	1
$u_t = u_{xxx}$		2	1
$u_t = u_{xxxx}$		2	2
$u_t = u_{xxxxx}$		2	3
$u_t + uu_x + u_{xxx} = 0$	KdV	1	2
$u_t + uu_x + u_{xx} + u_{xxxx} = 0$	KS	2	2

The challenge thus lies in approximating (1.2) so that (i) as many of the leading eigenvalues (and eigenvectors) as possible become accurately approximated, and (ii) the remaining (spurious) numerical eigenvalues are all located far out in the left half-plane, so as not to damage either the accuracy or the stability when using the MOL approach with a stiff ODE solver.

When using Galerkin (or tau) spectral methods—working with expansion coefficients rather than with node values as in the present pseudospectral (PS) approach—remedies have been discussed numerous times in the literature, e.g., [15], [23], and the references therein. However, especially in contexts involving variable coefficients and nonlinearities, the PS approach tends to be a lot more convenient.

In the next two sections of this paper, we summarize some approaches for resolving the problem with spurious eigenvalues when using the PS approach. We will note that an approach based on fictitious points (previously introduced for spectral methods in [13], in a slightly different context) is particularly effective, flexible, and simple to implement. In section 4, we discuss the same issues for some more general PDEs, in particular for the Kuramoto–Sivashinsky (KS) equation, and for some linearized versions of it. We note in section 5 that the issue of time-space corner singularities still needs more investigation, especially in the presence of nonlinearities. The example in section 6 illustrates this singularity issue, and also shows that the application of inhomogeneous boundary conditions (BCs) causes no further difficulties. Section 7 contains some concluding remarks.

2. Differentiation matrix (DM) approaches. With the node points denoted by $x_k,\ k = 0, 1, \ldots, n$, and the corresponding function values by u_k, the first derivative values u'_k can be approximated by means of a matrix×vector product

$$\begin{bmatrix} & & \\ & D^1 & \\ & & \end{bmatrix} \begin{bmatrix} u_0 \\ u_1 \\ \vdots \\ u_n \end{bmatrix} = \begin{bmatrix} u'_0 \\ u'_1 \\ \vdots \\ u'_n \end{bmatrix}.$$

Requiring that this formula becomes exact for all polynomials of degree n determines the differentiation matrix D^1 uniquely. This matrix can be computed at a cost of only four operations per entry by means of the explicit formula [27]

$$D^1_{j,k} = \begin{cases} \dfrac{a_j}{a_k(x_j - x_k)} & \text{if } j \neq k, \\ \displaystyle\sum_{\substack{i=0 \\ i\neq k}}^{n} \dfrac{1}{x_k - x_i} & \text{if } j = k, \end{cases} \qquad \text{where } a_k = \prod_{\substack{i=0 \\ i\neq k}}^{n} (x_k - x_i).$$

For higher derivatives, the corresponding DMs can be obtained by immediate matrix multiplication, i.e., $D^p = (D^1)^p$. However, several direct recursions have been found which give the entries of D^p both faster and in a more numerically stable manner. For different methods and/or variations, see, for example, [12], [14], [19], [35], [36], [37], [38]. In all the following discussions, we have used Chebyshev distributed nodes, i.e., $x_k = -L\ \cos\frac{\pi k}{n},\ k = 0, 1, 2, \ldots, n,$ in case of the interval $[-L, L]$. However, the results and conclusions become the same for similar choices, such as Legendre, Gegenbauer, or Jacobi distributions.

The immediate numerical discretization of (1.2) can be written as

$$\text{ODE:} \quad \left[\ D^3\ \right]_{n+1,n+1} \left[\ u\ \right]_{n+1} = \lambda \left[\ u\ \right]_{n+1}, \tag{2.1}$$

with

$$\text{BC:} \quad \begin{bmatrix} 1 & 0 & \ldots & 0 & 0 \\ 0 & 0 & \ldots & 0 & 1 \\ d_0 & d_1 & \ldots & d_{n-1} & d_n \end{bmatrix}_{3,n+1} \begin{bmatrix} u \end{bmatrix}_{n+1} = \begin{bmatrix} 0 \\ 0 \\ 0 \end{bmatrix}_3. \tag{2.2}$$

We have here also marked the sizes of the matrices and vectors. The most natural way to incorporate the first two BCs would be to simply remove the first and last rows and columns from D^3 and the first and last elements of u, leading to the eigenvalue problem $\widehat{D^3}\hat{u} = \lambda\hat{u}$ of size $(n-1) \times (n-1)$. Had there been no more BCs (as in the case for second derivatives using one condition at each end), this would have been fully satisfactory. However, we have here also a third BC. Its implementation is much less apparent, and forms the main topic of this present study.

Trefethen notes in [32, page 135] "There are two basic approaches to boundary conditions for spectral collocation methods: (I) *Restrict attention to interpolants that satisfy the boundary conditions*; or (II) *Do not restrict the interpolants, but add additional equations to enforce the boundary conditions*." We describe this second approach first, in subsection 2.1. Most recent work has concentrated on the first approach, discussed in subsection 2.2. We introduce then, in section 3, the fictitious point (FP) approach. This is very simple to implement and, as will be shown, lends itself especially well to the time stepping of PDEs with either homogeneous or inhomogeneous BCs.

2.1. Approach II: Elimination of an additional row and column. Merryfield and Shizgal [24] consider the possibility of adding suitable multiples of the last BC in (2.2) to the different rows in the ODE, so that also the second column of D^3 gets eliminated. The second unknown u_1 can, from this BC, be expressed in terms of the remaining unknowns:

$$u_1 = -\frac{1}{d_1} \sum_{i \neq 1} d_i u_i. \tag{2.3}$$

In order not to impose more relations than there are unknowns, we would then omit imposing the ODE at this second grid point location. The eigenvalue problem has then been reduced to size $(n-2) \times (n-2)$. We write this as

$$\widetilde{D_1^3} = \lambda\check{u}, \tag{2.4}$$

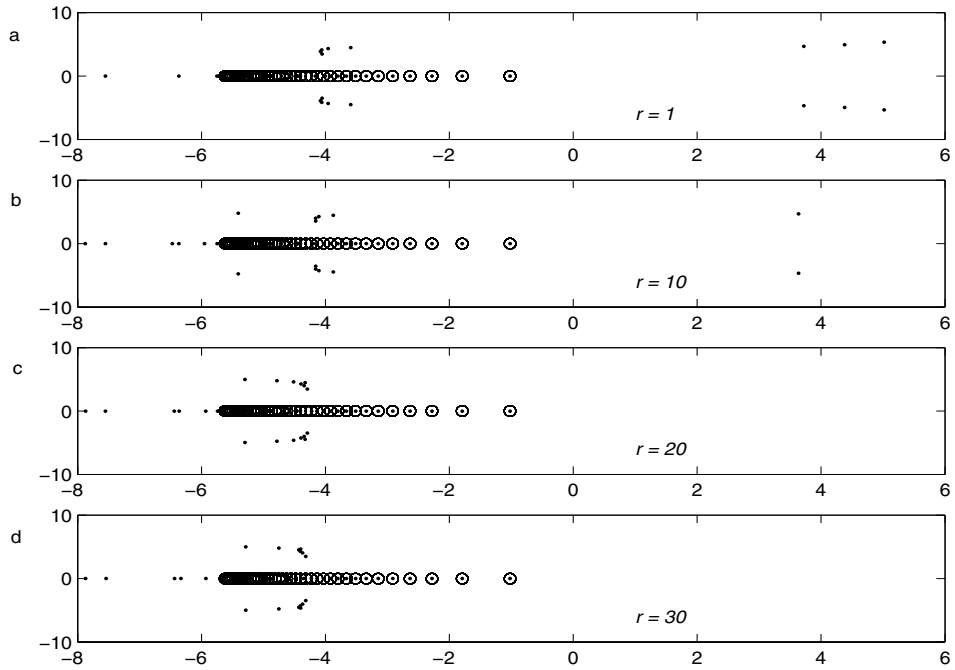

FIG. 2.1. *Complex spectra for the reduced matrix* $\check{D}_1^3$ *in the Mulholland approach, when the first and last row and column and also row and column* r, $r = 1, 10, 20, 30$, *have been eliminated. The axes have been scaled by* $x \to sign(x)\ \log_{10}(1 + |x|)$ *and similarly for* y (*in order to keep signs but compress large arguments*).

where the subscript "1" denotes that the second row and column are also eliminated (recalling that we count rows and columns starting with zero). Figure 2.1(a) (labeled $r = 1$) compares, in the case of $n = 40$ and $L = 1$, the eigenvalue distribution for (2.4) (marked by dots) against the first $n + 1$ analytic eigenvalues (marked by circles). As Merryfield and Shizgal first noted, the presence of several spurious eigenvalues far out in the right half-plane rules out this approach in the context of MOL time stepping.

Mulholland [26] generalized the approach of eliminating row 1 and column 1 to instead eliminating row r and column r, where $1 \le r \le n - 1$. Since the extra boundary condition appears at the left boundary, Merryfield and Shizgal's choice $r = 1$ is what first comes to mind. However, it transpires that the stability situation improves very much when r is increased. Figures 2.1(b), (c), (d) show the results with $r = 10, 20, 30$, respectively. Although the situation with r approaching n might appear satisfactory in the present case, there is something strange about eliminating a node in the Chebyshev grid far away from the boundary at which the extra condition had to be imposed. In fact, the generalization

$$u_r = -\frac{1}{d_r} \sum_{i \ne r} d_i u_i \tag{2.5}$$

of (2.3) becomes problematic because the weights d_i are oscillatory and decay rapidly in magnitude with increasing r. Figure 2.2 shows these in the case of $L = 1$ and $n = 20$. Some coefficients d_i/d_r in (2.5) become much larger than one, and small oscillations in u_i, $i < r$, get strongly amplified in the computed value of u_r. The

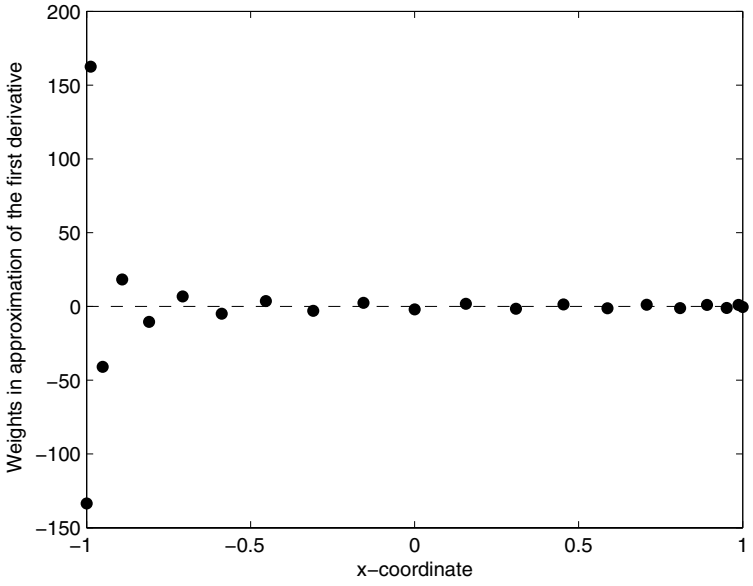

FIG. 2.2. *Weights d_i when the first derivative is approximated at the left boundary of a* 21*-node Chebyshev-spaced grid.*

reason the methodology still works, even as r is increasing, is that the resulting errors in u_r occur close to the right boundary, and the general character of solutions to (1.1) is that all modes are transported towards this right boundary and become completely absorbed there—the faster the higher the mode is. It thus would appear that the Mulholland approach will work only for very special PDEs. In fact, it fails entirely for the KS equation, which we will consider in section 4.

2.2. Approach I: Modify the DM to incorporate the boundary information. Determining the DM for collocation at $x_0,\ x_1, \ldots, x_n$ with a polynomial $p_n(x)$ over $[-1, 1]$ and then enforcing $u(-1) = u(1) = 0$ leads to the same DM as one would get if one considered only polynomials of the form $(x + 1)(x - 1)p_{n-2}(x)$ and collocated only over the internal nodes $x_1, \ldots, x_{n-1}$. In order to also enforce $u_x(-1) = 0$, we can collocate over the interior nodes with a polynomial of the form $(x+1)^2(x-1)p_{n-2}(x)$. This type of approach was taken by Funaro and Heinrichs [16], later independently by Huang and Sloan [18], and again by Heinrichs [17]. In these cases, closed form expressions for the resulting DMs were obtained. Trefethen [32, page 146] describes another approach which, for arbitrary node distributions, gives the desired DM from standard ones in just a few matrix operations. Figure 2.3(a), showing its eigenvalues, should be compared to Figure 2.1. The spurious eigenvalues are located as advantageously as in any of the previous cases from Mulholland's method, but without the need to discard the governing equation at any one of the interior grid points. One of the referees of the present paper proposed the following procedure: with $\underline{u} = [u(-1), u_1, u_2, \ldots, u_{n-1}, u(1)]^T$, form $D^1\underline{u}$, set its first component to $u'(-1)$, and then apply D^2 to get an approximation for u_{xxx} that incorporates the given values of $u(-1)$, $u(1)$, and $u'(-1)$. This procedure, which is particularly simple to implement in case of nonhomogeneous BC, gives results that are only very slightly

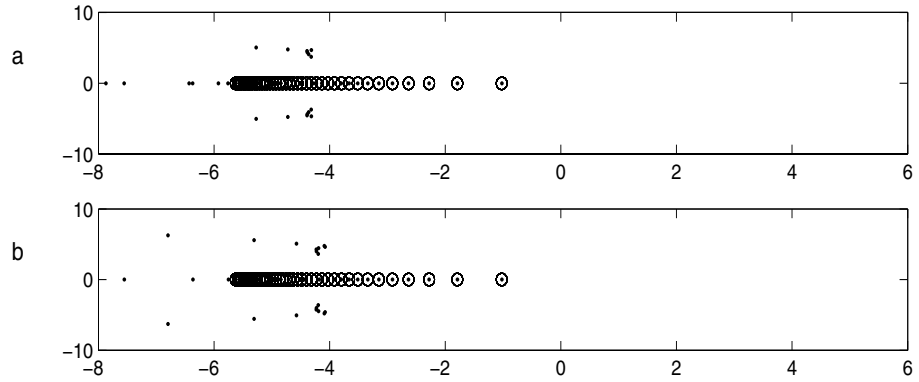

FIG. 2.3. *Complex spectrum for the same test case as in Figure* 2.1. (a) *Collocation with a polynomial of the form* $(x+1)^2(x-1)p_{n-2}(x)$. *This will agree with the FP method described in section* 3. (b) *Last method described in section* 2.2.

different from the method just mentioned (as seen in Figure 2.3(b)).

None of the methods/implementations that have just been mentioned combine all of the following desirable features:

(i) easy implementation;

(ii) easy generalization to nonhomogeneous cases;

(iii) ability to handle Robin-type BCs (involving linear combinations of values and derivatives, in place of values and/or derivatives);

(iv) ability to impose BCs on staggered-type grids (where the actual boundary location does not coincide with a grid point).

3. Fictitious point approach. Although for simplicity, our description will not be the most general, the FP approach will be seen to meet all the four criteria that were just noted.

Since we in our model problem (1.2) have one more BC than can be imposed by just fixing the values for $u(x_0)$ and $u(x_n)$, we introduce an additional grid point at some arbitrary location x_{FP}. When evaluating the matrix D^3, for example, by the algorithm in [37], this point is included just like $x_0, \ldots, x_n$. The extra BC can be expressed as a linear combination of node values:

$$\begin{bmatrix} d_{FP} & d_0 & d_1 & \ldots & d_{n-1} & d_n \end{bmatrix}_{n+2} \begin{bmatrix} u \end{bmatrix}_{n+2} = 0.$$

Since finding these weights requires the computation of only one global FD stencil (rather than a full DM), the algorithm in [12] is particularly suitable for this task. Multiples of $[d_{FP}\ d_0\ d_1\ \ldots\ d_{n-1}\ d_n]$ are next subtracted from D^3 in order to eliminate all weights at x_{FP}. The two BCs for $u(x_0)$ and $u(x_n)$ are implemented as before, i.e., we omit the first and last row and column of D^3. The key to this approach is that, apart from possible rounding errors, the resulting $\widetilde{D^3}$ matrix becomes completely independent of our choice for x_{FP}. The reason for this is that introducing this point and then eliminating all weights at it can be seen as a particularly convenient way to find the same DM as before, i.e., corresponding to collocating with polynomials of

the form

$$P(x) = (x+1)^2(x-1)p_{n-2}(x). \tag{3.1}$$

The equivalence just mentioned can be explained in more detail as follows: Data values $u_0 = 0,\ \{u_i, i = 1, 2, \ldots, n-1\},\ u_n = 0$ at node locations $x_0 = -1,\ \{x_i, i = 1, 2, \ldots, n-1\},\ x_n = 1$ determine uniquely the polynomial $P(x)$ in (3.1). We next choose an additional point x_{FP} and evaluate $u_{FP} = P(x_{FP})$. If we extend the data set above with the value u_{FP} at location x_{FP}, it will then consist of $n+2$ points, and it therefore determines a unique interpolating polynomial of degree $n+1$. This polynomial must be identical to $P(x)$. The FP approach provides the exact value for any derivative of this polynomial, at any location, i.e., its results must agree exactly with those obtained by immediate use of (3.1). The value we happened to have chosen for x_{FP} did not affect $P(x)$ (which was determined before x_{FP} was introduced), and it could therefore not in any way have influenced the outcome of the FP method.

The general idea of introducing one (or more) temporary grid points outside an interval is not new. It has long been used to implement Neumann conditions in connection with low order FD methods (e.g., [30, page 32]); other contexts include domain decomposition, block-PS methods [7], [8], and the "enslaving" idea for FD schemes [21]. In all these cases, the final computational result will depend on where the extra point(s) are located. The expression "fictitious point" was first used in [13], in a situation where the point truly vanished in the sense that not even its temporary location left any remaining trace behind. We use here the term FP in that sense. These points can just as well be placed inside a computational domain as outside it.

4. The Kuramoto–Sivashinsky equation. The KS equation can be written

$$u_t = -u\ u_x - u_{xx} - u_{xxxx}. \tag{4.1}$$

It features some similarities with Burgers' equation

$$u_t = -u\ u_x + u_{xx} \tag{4.2}$$

but is more interesting in several respects. In (4.2), the dissipative term u_{xx} counteracts the effects of steepening caused by the nonlinear term uu_x, and solutions typically evolve into pulses which travel while decaying. In (4.1), the u_{xx} term (in conjunction with the time derivative) amounts to the backwards heat equation, which is unstable for all modes. Inclusion of the u_{xxxx} term causes high modes to become dampened while low modes remain unstable. The uu_x term causes again a steepening of waves, with the effect that unstable modes of sufficient height get brought over to the stable higher-frequency regime. The KS equation models numerous phenomena in physics [34] and is a frequently used model equation for chaotic dynamics [20], [29].

A very brief Fourier-PS MATLAB code, slightly modified from [33], has been used to produce Figure 4.1. This shows how the small initial disturbance

$$u(x,0) = \begin{cases} 0.1\ \sin^2(x/2), & -12\pi < x < -10\pi, \\ 0 & \text{otherwise} \end{cases} \tag{4.3}$$

over the periodic domain $[-16\pi, 16\pi]$ causes chaotic structures to emerge.

4.1. A linear model equation. In preparation for introducing a nonperiodic PS code for the KS equation, we next consider the linear problem

$$u_t = -u_{xx} - u_{xxxx} \tag{4.4}$$

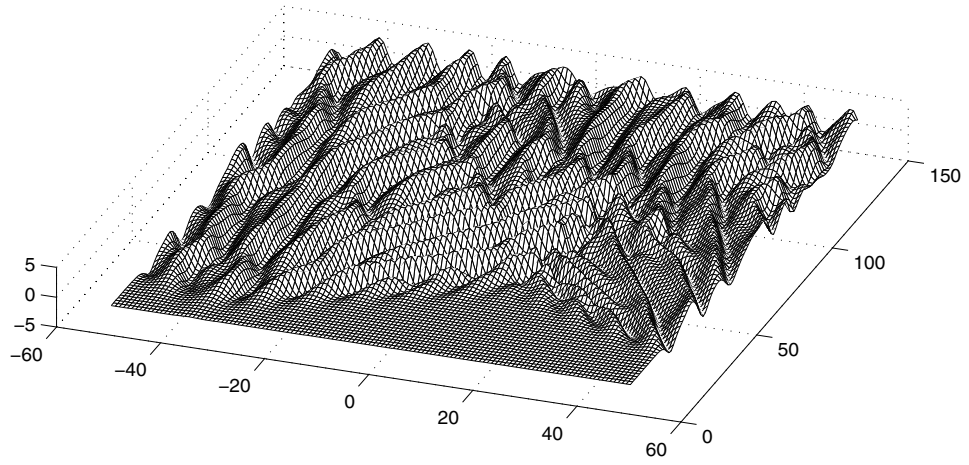

FIG. 4.1. *Periodic solution to the KS equation* (4.1) *with initial condition* (*IC*) (4.3) *computed with a periodic PS method using* 128 *points in space.*

with BCs

$$u(\pm L, t) = 0,\ u_x(\pm L, t) = 0. \tag{4.5}$$

If we at first limit ourselves still further to

$$u_t = -u_{xx} \tag{4.6}$$

with BC $u(\pm L) = 0$, the corresponding eigenvalues become

$$\lambda_k = \left[\frac{k\pi}{2L}\right]^2, \quad k = 1, 2, 3, \ldots,$$

and for

$$u_t = -u_{xxxx} \tag{4.7}$$

with BC (4.5), they become $\lambda_k = -\left(\frac{\rho_k}{2L}\right)^4$, where ρ_k is the kth positive root to $\cos(\rho) \cdot \cosh(\rho) = 1$, i.e.,

$$\lambda_k \approx -\left[\frac{(k + \frac{1}{2})\pi}{2L}\right]^4, \quad k = 1, 2, 3, \ldots .$$

The PS approach to (4.6) features all real and positive eigenvalues, as seen in Figure 4.2(a) for the case of $L = 20$ and $n = 10, 20, 30, \ldots, 80$. The lowest eigenvalues are very accurate, whereas the higher (spurious) ones become very large. Figure 4.2(b) shows similarly the FP PS method's eigenvalues for (4.7). These are all negative—again with spurious ones far away. One might have guessed that the FP-computed eigenvalues to the combined equation (4.4) would feature spurious eigenvalues both to the right and to the left (and, if so, causing maybe insurmountable time stepping difficulties). However, as Figure 4.2(c) shows, they are all far out in the left half-plane. Although the equation that gives the exact eigenvalues to (4.4) is too complicated to be practical to work with, they can nevertheless be computed accurately. The lower eigenvalues appear in close pairs, as can be seen in the tabulation along the top edge of Figure 4.3. The figure also shows graphically the errors in FP-type PS approximations based on increasingly fine Chebyshev distributions.

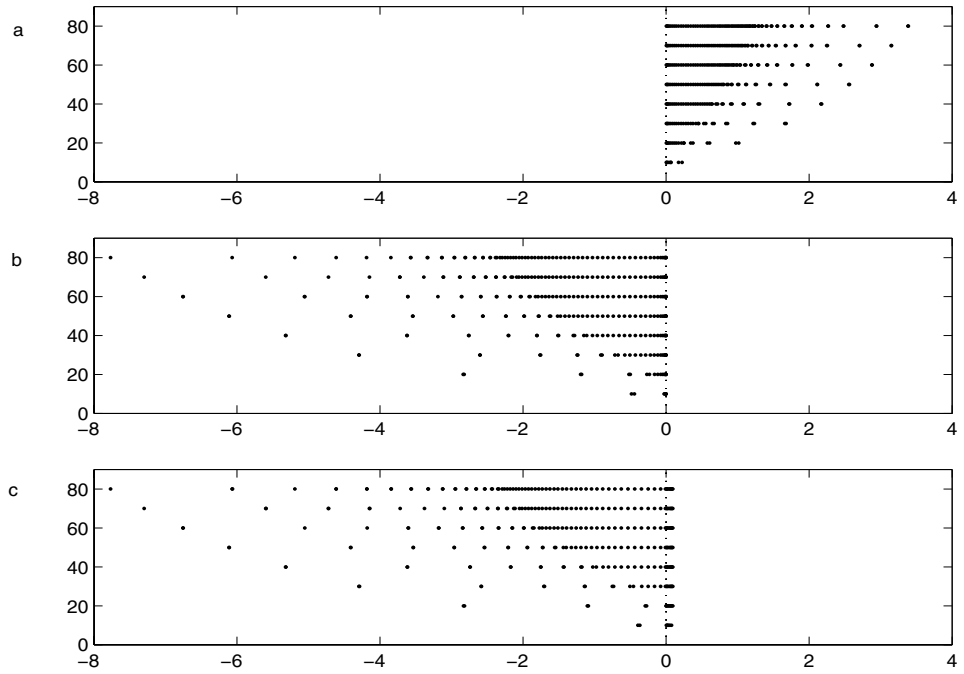

FIG. 4.2. *Eigenvalues* (*all real*) *in cases of* $N = 10, 20, 30, \ldots, 80$ *for* (a) *equation* (4.6), (b) *equation* (4.7), *and* (c) *equation* (4.4). *The scaling in the horizontal direction is the same as described in the caption for Figure* 2.1.

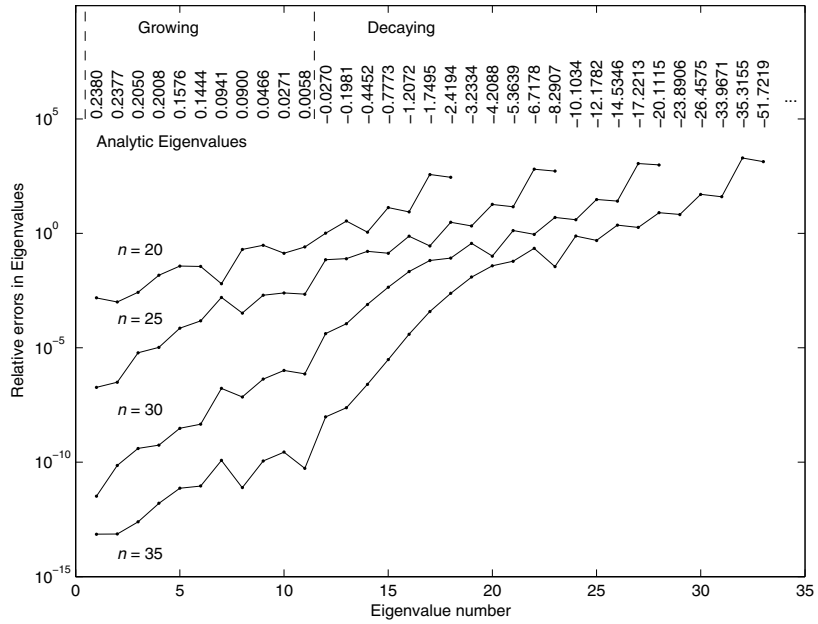

FIG. 4.3. *Relative errors in different eigenvalues for the linearized KS equation* (4.4) (*in the case of* $L = 20$).

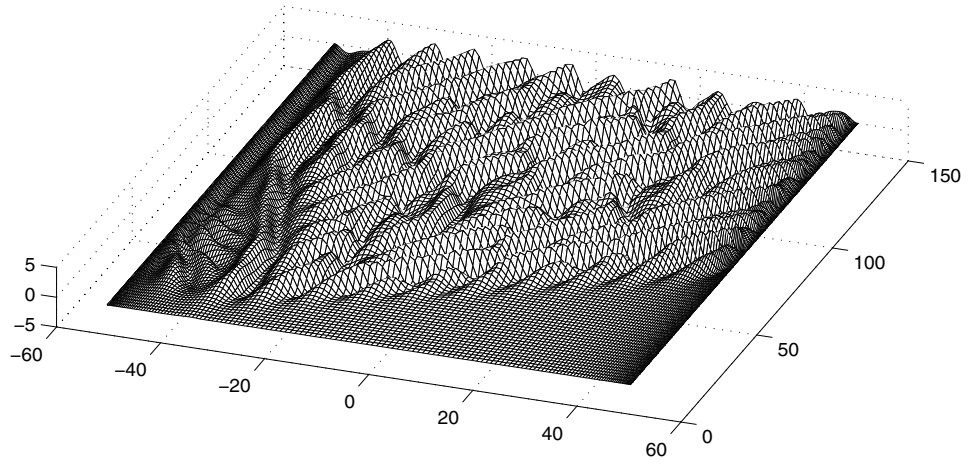

FIG. 4.4. *Nonperiodic solution to the KS equation* (4.1)*, computed by the FP PS method.*

4.2. Numerical solution of the nonperiodic KS equation. The FP PS method, as just described, has been implemented for solving the KS equation (4.1) with the nonperiodic BC $u(\pm L, t) = 0,\ u_x(\pm L, t) = 0$. With again $L = 16\pi$ and the IC (4.3), Figure 4.4 shows the resulting time evolution.

In this calculation, the time stepping (again over $0 \le t \le 150$) was performed with the 2-stage fourth order accurate Hammer–Hollingsworth implicit Runge–Kutta scheme. However, any standard stiff ODE solver should also have worked perfectly well. According to comparisons in [22], an LI (linearly implicit) scheme or an ETD (exponential time differencing) scheme would likely have been a more effective choice. The former have a long history, and were recently surveyed, for example, in [1] and [5], while Runge–Kutta-based LI schemes are considered in [28]. It should, however, be noted that Boyd [3, pages 267–269] warns against their use for certain nonlinear wave equations. ETD schemes were introduced independently several times [31], [2], [25], and [6], with a stability problem resolved in [22]. In Figure 4.4, we see again a chaotic solution that reaches approximately the same amplitude as in the periodic case. However, both quantitative and qualitative differences can be spotted compared to the periodic case that was previously displayed in Figure 4.1.

5. Time-space corner singularities. In applications leading to IBV problems, ICs and BCs typically come from different physical considerations. In order for the solutions to the PDE not to feature singularities in the time-space corners where ICs and BCs meet, an infinite number of compatibility conditions need to hold, as explored by Flyer and collaborators [4], [9], [10], [11]. For (1.1), these were analyzed in detail in [10]. Figure 5.1 shows for $k = 1$ and $k = 2$ the structure of the solutions

(5.1)
$$u_k(x,t) = t^k \left\{ {}_1F_2\left(-k, \left\{\frac{1}{3}, \frac{2}{3}\right\}, -\frac{x^3}{27t}\right) - \frac{x^2}{2t^{2/3}} \frac{\Gamma(k+1)}{\Gamma(k+\frac{1}{3})}\ {}_1F_2\left(\frac{2}{3} - k, \left\{\frac{4}{3}, \frac{5}{3}\right\}, -\frac{x^3}{27t}\right)\right\}$$

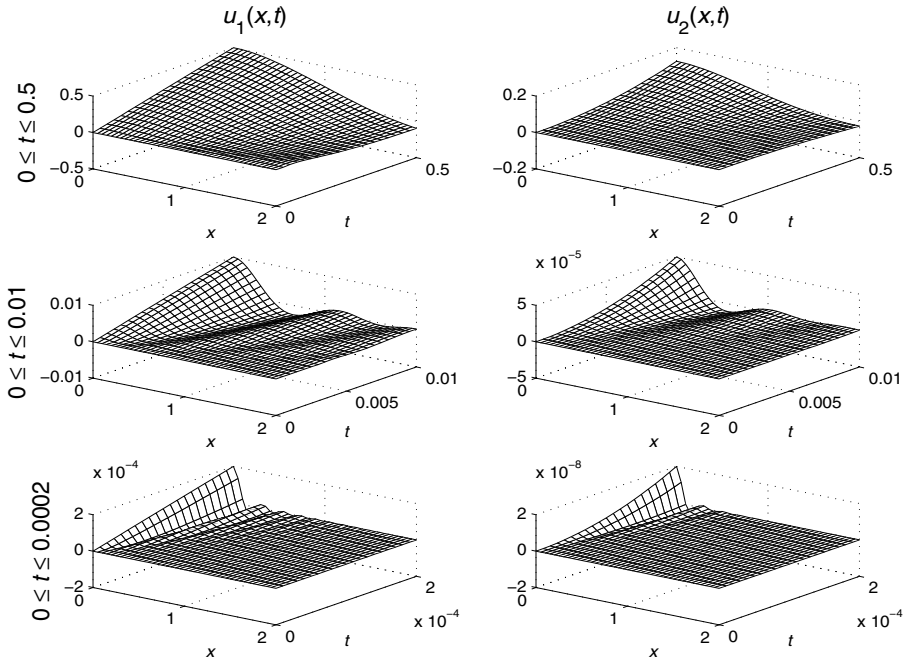

FIG. 5.1. *The corner functions $u_1(x,t)$ and $u_2(x,t)$ for* (5.2)*, displayed over progressively shorter initial time intervals.*

near the origin for the quarter-plane problems

$$
\text{(5.2)} \qquad \begin{cases} \text{PDE} & u_t = u_{xxx}, \\ \text{IC} & u(x,0) = 0, \\ \text{BC} & \begin{cases} u(t,0) &= t^k, \\ u_x(t,0) &= 0, \end{cases} \quad k = 0,1,2,\ldots; \;\; u(t,\infty) = 0, \end{cases}
$$

$x \ge 0$, $t \ge 0$. For the BCs $u(t,0) = 0, \;\; u_x(t,0) = t^k$, we denote the corresponding quarter-plane solutions by $v_k(x,t)$:

$$
v_k(x,t) = t^{k+\frac{1}{3}} \left\{ {}_1F_2\left(-k, \left\{\frac{2}{3}, \frac{4}{3}\right\}, -\frac{x^3}{27t}\right) - \frac{x^2}{2t^{2/3}} \frac{\Gamma(k+1)}{\Gamma(k+\frac{2}{3})} \, {}_1F_2\left(\frac{1}{3} - k, \left\{\frac{4}{3}, \frac{5}{3}\right\}, -\frac{x^3}{27t}\right) \right\}.
$$

The top row of subplots in Figure 5.1 shows seemingly very smooth analytic solutions, for which one would not expect any numerical difficulties. No amount of "zooming in" (uniformly in x and t) near the origin in the (x,t)-plane will visually reveal any irregularities. However, if we increase the graphical resolution in time only, the lower subplots reveal the presence of transient fine structures which accurate numerics would also need to resolve. A typical numerical approach, as explained in some detail for convective-diffusive equations in [9], would be to subtract an appropriate combination of different *corner singularity functions* before an FP PS numerical method is applied to the remaining problem.

The issue of corner singularities in the time-space domain was little noted before the advent of spectral methods, since the truncation errors of finite difference and finite element methods tended to dominate over them. However, when using PS methods,

corner-induced errors can easily dominate over other errors with many orders of magnitude. In the present test case for the KS equation (4.1), all space derivatives of the IC (4.3) and time derivatives of the BC (4.5) are zero in the corners, and this issue did not arise. However, it needs to be noted that it is one that has to be considered in most spectral IBV calculations. The precise form of the corner singularity functions for most higher order PDEs (such as (4.4) and (4.1)) remains to be investigated. For cases when they cannot be obtained in convenient closed form, it was noted in [9] that a simple change of variables makes their numerical computation straightforward.

6. Inhomogeneous boundary conditions. The description of the FP approach in section 3 applies entirely unchanged also to the case of inhomogeneous BCs. As an example, we consider the case illustrated in the center left subplot of Figure 5.1, i.e., we use the FP method to numerically solve

$$\text{(6.1)} \qquad \begin{cases} \text{PDE} & u_t = u_{xxx}, \\ \text{IC} & u(x,0) = 0, \\ \text{BC} & u(0,t) = t,\ u_x(0,t) = 0,\ u(2,t) = \left\{ \begin{array}{c} \text{values from the ana-} \\ \text{lytic solution (5.1)} \end{array} \right\} \end{cases}$$

for $0 \le t \le 0.01$. The resulting solution should agree exactly with the $k = 1$ case of (5.1). Figure 6.1(a) shows the result on a 20-node Chebyshev grid with the time stepping, this time carried out with one of MATLAB's standard stiff ODE solvers (ode15s). Part (b) of the figure shows the error compared to the analytic solution. At the very first moments, extremely high frequency transients emerge from the origin (where the ICs and BCs meet) and then race to the right across the spatial domain. After they have done so, and have "died down" at the right boundary, the numerical solution features a very high accuracy. As we noted above, these initial transients at first contain frequencies that are too high for any computational grid, and the error they cause

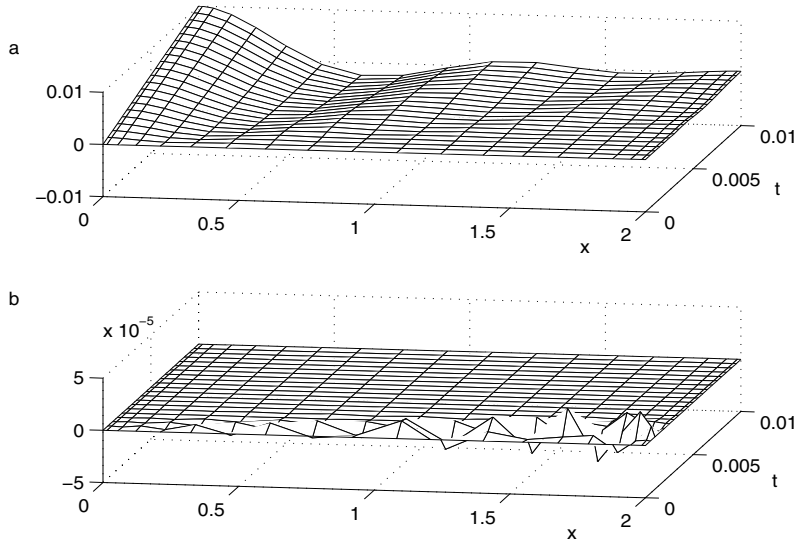

FIG. 6.1. *The $u_1(x,t)$ corner function for $u_t = u_{xxx}$.* (a) *Numerical FP solution on a* 20*-node Chebyshev grid.* (b) *The error compared to the analytic solution.*

can easily dominate all other errors by several orders of magnitude. It depends on the application whether or not accurate resolution of initial transients is important.

7. Conclusions. High order IBV problems can require several conditions at each boundary. When using Chebyshev-type PS approximations in space, it has in the past not been clear how best to implement these conditions in order to obtain good accuracy, stability, flexibility, and simplicity. The present FP approach has been shown to meet such requirements. Demonstration cases have included the KS equation as well as the dispersive wave equation $u_t = u_{xxx}$ with inhomogeneous boundary conditions. As with other Chebyshev-type PS methods, the DMs in the FP approach are not particularly close to being normal matrices. However, they are close enough that eigenvalue analysis accurately describes actual stability under time stepping. With the very high accuracy that is now easily reachable also for high order IBV problems, the singularities that such equations generally have at time-space corners (where ICs and BCs meet) will need to be taken into account, especially in computations over short times.

REFERENCES

[1] U. M. Ascher, S. J. Ruuth, and B. T. R. Wetton, *Implicit-explicit methods for time-dependent partial differential equations*, SIAM J. Numer. Anal., 32 (1995), pp. 797–823.

[2] G. Beylkin, J. M. Keiser, and L. Vozovoi, *A new class of time discretization schemes for the solution of nonlinear PDEs*, J. Comput. Phys., 147 (1998), pp. 362–387.

[3] J. P. Boyd, *Chebyshev and Fourier Spectral Methods*, 2nd ed., Dover, New York, 2000.

[4] J. P. Boyd and N. Flyer, *Compatibility conditions for time-dependent partial differential equations and the rate of convergence of Chebyshev and Fourier spectral methods*, Comput. Methods Appl. Mech. Engrg., 175 (1999), pp. 281–309.

[5] C. Canuto, M. Y. Hussaini, A. Quarteroni, and T. A. Zang, *Spectral Methods in Fluid Dynamics*, Springer-Verlag, Berlin, 1988.

[6] S. M. Cox and P. C. Matthews, *Exponential time differencing for stiff systems*, J. Comput. Phys., 176 (2002), pp. 430–455.

[7] T. A. Driscoll and B. Fornberg, *A block pseudospectral method for Maxwell's equations:* I. *One-dimensional case*, J. Comput. Phys., 140 (1998), pp. 47–65.

[8] T. A. Driscoll and B. Fornberg, *Block pseudospectral methods for Maxwell's equations* II: *Two-dimensional, discontinuous-coefficient case*, SIAM J. Sci. Comput., 21 (1999), pp. 1146–1167.

[9] N. Flyer and B. Fornberg, *Accurate numerical resolution of transients in initial-boundary value problems for the heat equation*, J. Comput. Phys., 184 (2003), pp. 526–539.

[10] N. Flyer and B. Fornberg, *On the nature of initial-boundary value solutions for dispersive equations*, SIAM J. Appl. Math., 64 (2003), pp. 546–564.

[11] N. Flyer and P. N. Swarztrauber, *The convergence of spectral and finite difference methods for initial-boundary value problems*, SIAM J. Sci. Comput., 23 (2002), pp. 1731–1751.

[12] B. Fornberg, *Generation of finite difference formulas on arbitrarily spaced grids*, Math. Comp., 51 (1988), pp. 699–706.

[13] B. Fornberg, *A Practical Guide to Pseudospectral Methods*, Cambridge University Press, Cambridge, UK, 1996.

[14] B. Fornberg, *Calculation of weights in finite difference formulas*, SIAM Rev., 40 (1998), pp. 685–691.

[15] D. R. Gardner, S. A. Trogdon, and R. W. Douglas, *A modified tau spectral method that eliminates spurious eigenvalues*, J. Comput. Phys., 80 (1989), pp. 137–167.

[16] D. Funaro and W. Heinrichs, *Some results about the pseudospectral approximation of one-dimensional fourth-order problems*, Numer. Math., 58 (1990), pp. 399–418.

[17] W. Heinrichs, *Spectral approximation of third-order problems*, J. Sci. Comput., 14 (1999), pp. 275–289.

[18] W. Huang and D. M. Sloan, *The pseudospectral method for third-order differential equations*, SIAM J. Numer. Anal., 29 (1992), pp. 1626–1647.

[19] W. Huang and D. M. Sloan, *The pseudospectral method for solving differential eigenvalue problems*, J. Comput. Phys., 111 (1994), pp. 399–409.

[20] J. M. Hyman and B. Nicolaenko, *The Kuramoto–Sivashinsky equation: A bridge between partial differential equations and dynamical systems*, Phys. D, 18 (1986), pp. 113–126.
[21] D. A. Jones, L. G. Margolin, and A. C. Poje, *Enslaved finite difference schemes for nonlinear dissipative PDEs*, Numer. Methods Partial Differential Equations, 12 (1996), pp. 13–40.
[22] A.-K. Kassam and L. N. Trefethen, *Fourth-order time-stepping for stiff PDEs*, SIAM J. Sci. Comput., 26 (2005), pp. 1214–1233.
[23] G. B. McFadden, B. T. Murray, and R. F. Boisvert, *Elimination of spurious eigenvalues in the Chebyshev tau spectral method*, J. Comput. Phys., 91 (1990), pp. 228–239.
[24] W. J. Merryfield and B. Shizgal, *Note: Properties of collocation third-derivative operators*, J. Comput. Phys., 105 (1993), pp. 182–185.
[25] D. R. Mott, E. S. Oran, and B. van Leer, *A quasi-steady state solver for the stiff ordinary differential equations of reaction kinetics*, J. Comput. Phys., 164 (2000), pp. 407–428.
[26] L. S. Mulholland, *The Eigenvalues of Third-Order Chebyshev Pseudospectral Differentiation Matrices*, Mathematics Research Report, 6, University of Strathclyde, Glasgow, UK, 1995.
[27] K. L. Nielsen, *Methods in Numerical Analysis*, MacMillan, New York, 1956.
[28] S. J. Ruuth, *Implicit-explicit Runge–Kutta methods for time dependent partial differential equations*, Appl. Numer. Math., 25 (1997), pp. 151–167.
[29] B. I. Shraiman, *Order, disorder, and phase turbulence*, Phys. Rev. Lett., 57 (1986), pp. 325–328.
[30] G. D. Smith, *Numerical Solution of Partial Differential Equations*, Oxford University Press, New York, 1965.
[31] A. Taflove, *Computational Electrodynamics: The Finite-Difference Time-Domain Method*, Artech House, Boston, 1995.
[32] L. N. Trefethen, *Spectral Methods in MATLAB*, SIAM, Philadelphia, 2000.
[33] L. N. Trefethen, 1-*page,* 1-*second Matlab ETDRK*4 *code for Kuramoto–Sivashinsky equation*, available online from http://web.comlab.ox.ac.uk/oucl/work/nick.trefethen/.
[34] L. N. Trefethen, *The PDE Coffee Table Book*, in preparation.
[35] J. R. Quan and C. T. Chang, *New insights in solving distributed system equations by the quadrature methods*—I., Comput. Chem. Engrg., 13 (1989), pp. 779–788.
[36] J. R. Quan and C. T. Chang, *New insights in solving distributed system equations by the quadrature methods*—II., Comput. Chem. Engrg., 13 (1989), pp. 1017–1024.
[37] J. A. C. Weideman and S. C. Reddy, *A MATLAB differentiation matrix suite*, ACM Trans. Math. Software (TOMS), 26 (2000), pp. 465–519. (See also http:/dip.sun.ac.za/˜weideman/research/differ.html.)
[38] B. D. Welfert, *Generation of pseudospectral differentiation matrices* I, SIAM J. Numer. Anal., 34 (1997), pp. 1640–1657.